

Article

# Vibrational Spectroscopic Identification of the $[\text{AlCl}_2]^+$ Cation in Ether-Containing Liquid Electrolytes

Gabriela P. Gomide <sup>1,\*</sup>, Wagner A. Alves <sup>1,\*</sup>  and Andrzej Eilmes <sup>2,\*</sup> 

<sup>1</sup> Núcleo de Espectroscopia e Estrutura Molecular (NEEM), Departamento de Química, Instituto de Ciências Exatas, Universidade Federal de Juiz de Fora, Juiz de Fora 36036-900, MG, Brazil

<sup>2</sup> Faculty of Chemistry, Jagiellonian University, Gronostajowa 2, 30-387 Kraków, Poland

\* Correspondence: wagner.alves@ufjf.br (W.A.A.); eilmes@chemia.uj.edu.pl (A.E.);

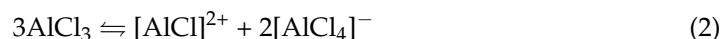
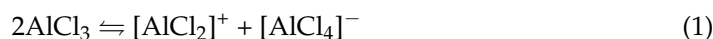
Tel.: +55-32-2102-3310 (W.A.A.); +48-12-6862377 (A.E.)

**Abstract:** A Raman and IR study of  $\text{AlCl}_3$ -based ethereal solutions is here presented and aims at identifying the  $[\text{AlCl}_2]^+$  cation, which has been so far unambiguously characterized by  $^{27}\text{Al}$  NMR spectrometry. To do that, experimental–theoretical vibrational spectroscopy was so employed, and the data are interpreted successfully. As a known amount of water is added to the tetrahydrofuran (THF)-containing electrolyte, a Raman band at  $271\text{ cm}^{-1}$  has its intensity increased along with the most intense band of  $[\text{AlCl}_4]^-$ , and such behavior is also seen for a band at  $405\text{ cm}^{-1}$  in the IR spectra. New bands at around  $420$  and  $400\text{ cm}^{-1}$  are observed in both Raman and IR spectra for the tetraglyme (G4)-based systems. The  $[\text{AlCl}_2(\text{THF})_4]^+$  complex, in the *cis* and *trans* forms, is present in the cyclic ether, while the *cis*- $[\text{AlCl}_2(\text{G4})]^+$  isomer is identified in the acyclic one.

**Keywords:** vibrational spectroscopy; aluminum chloride; ethereal liquid electrolytes

## 1. Introduction

Ethereal aluminum chloride solutions have been used in Al electrodeposition baths since the investigation performed by Couch and Brenner in 1952 [1]. Most recently (2014), the addition of magnesium chloride to those systems allowed researchers to easily synthesize the first Mg battery electrolyte with all-inorganic salts, termed the magnesium aluminum chloride complex (MACC) [2]. Various Mg(II) complexes and  $[\text{AlCl}_4]^-$  have been identified in this electrolyte [3–7], but the  $\text{MgCl}_2:\text{AlCl}_3$  ratio must be very well tuned in order to avoid the presence of  $[\text{AlCl}_2]^+$ , which seems to be responsible for corrosion of the Mg anode [8]. Not surprisingly therefore, such a cation and  $[\text{AlCl}]^{2+}$  have been proposed in  $\text{AlCl}_3$ -based ethereal systems in accordance with the reactions (1) and (2):



$^{27}\text{Al}$  NMR spectrometry has been widely used in the study of aqueous and non-aqueous solutions of aluminum salts. For instance, Nöth and coworkers [9] investigated  $\text{AlCl}_3$ /tetrahydrofuran (THF) solutions and three distinct peaks were identified: the most intense one at 64 ppm was related to pentacoordinated Al ( $\text{AlCl}_3 \cdot 2\text{THF}$ ), whereas a sharp line at 103 ppm resulted from the presence of a tetracoordinated species ( $[\text{AlCl}_4]^-$ ); a rather broad signal at around 19 ppm was interpreted on the basis of a hexacoordinated Al environment, which could be either  $[\text{AlCl}_2(\text{THF})_4]^+$  or  $[\text{AlCl}(\text{THF})_5]^{2+}$ . Replacing the solvent for mono-, di- and triglyme, only the sharp peak at 103 and a broad one at 25 ppm were detected. Those authors concluded that  $\text{AlCl}_3$  dissociation into  $[\text{AlCl}_4]^-$  and solvated  $[\text{AlCl}_2]^+$  and/or  $[\text{AlCl}]^{2+}$  increases as a function of the ether chelating effect. As expected, the  $^{27}\text{Al}$  NMR spectrum reported by Bieker and colleagues [8] for an  $\text{AlCl}_3$ /tetraglyme (G4) solution showed the two same signals, but the corresponding Raman spectrum revealed



**Citation:** Gomide, G.P.; Alves, W.A.; Eilmes, A. Vibrational Spectroscopic Identification of the  $[\text{AlCl}_2]^+$  Cation in Ether-Containing Liquid Electrolytes. *Molecules* **2024**, *29*, 5377. <https://doi.org/10.3390/molecules29225377>

Academic Editor: Francesco Crea

Received: 23 October 2024

Revised: 7 November 2024

Accepted: 12 November 2024

Published: 14 November 2024



**Copyright:** © 2024 by the authors. Licensee MDPI, Basel, Switzerland. This article is an open access article distributed under the terms and conditions of the Creative Commons Attribution (CC BY) license (<https://creativecommons.org/licenses/by/4.0/>).

only the presence of the tetrahedral anion. Similar vibrational spectroscopic results were reached by Kitada et al. [10], who also investigated the electrochemical properties of  $\text{AlCl}_3$  solutions in selected glymes. However, the structures of the  $[\text{AlCl}_2(\text{glyme})_n]^+$  complexes were based on the  $^{27}\text{Al}$  NMR data reported by other researchers [9].

So far, one can notice that  $[\text{AlCl}_4]^-$  has been easily identified in the Raman and IR spectra, in contrast to the cationic species. Derouault and Forel [11] synthesized the solid  $\text{AlCl}_3 \cdot \text{THF}$  and  $\text{AlCl}_3 \cdot 2\text{THF}$  compounds, and the vibrational analysis suggested that the former has a molecular structure, whereas the latter may be described as an  $[\text{AlCl}_2(\text{THF})_4]^+$ ,  $[\text{AlCl}_4]^-$ -type ionic arrangement. At the same year, Derouault and coauthors [12] spectroscopically investigated  $\text{AlCl}_3$  solutions in THF and in THF–dichloromethane mixtures. Owing to the use of a visible radiation laser, the Raman spectra were strongly disturbed by fluorescence, and so  $\text{AlCl}_3 \cdot 2\text{THF}$  and  $[\text{AlCl}_4]^-$  were the only species identified. On the other hand, weak signals near 440 and 360  $\text{cm}^{-1}$  were observed in the IR spectra and related to the  $[\text{AlCl}_2(\text{THF})_4]^+$  cation. Curiously, the absorption spectra are shown up to 300  $\text{cm}^{-1}$ , even though those authors have also employed polyethylene windows.

By using a near-IR radiation laser, Alves et al. [13] have recorded fluorescence-free Raman spectra of  $\text{AlCl}_3$  solutions in THF. Despite this advantage, the spectra were also characterized by the neutral and anionic species. Hence, we decide in this work to acquire Raman spectra with laser power equal to 1W, which is twice larger than the one previously used, aiming at identifying the cationic species in ethereal solvents with different coordinating abilities. The IR technique is also combined to Raman data in order to discuss aspects related to molecular isomerism. All experiments are supplemented by quantum chemical (QC) calculations employing density functional theory (DFT) and ab initio molecular dynamics (AIMD) simulations, and it is expected that information drawn from this study may be useful for the advance in the development of electrolytes employed in rechargeable Al(III) and Mg(II) batteries.

## 2. Results

### 2.1. Experimental Spectra

#### 2.1.1. $\text{AlCl}_3$ -THF System

The interaction of THF with  $\text{AlCl}_3$  is typically evidenced in the Raman spectrum by the bands at 858, 927 and 1042  $\text{cm}^{-1}$ , which arise from the perturbation provoked by the solute to the  $\nu_{\text{CO}} + \nu_{\text{CC}}$  stretching vibrations of the ether. These features have been observed in the present work, but considering that they were previously discussed in detail [13] and such wavenumbers had already been reported by other authors [12], the spectral range 1100–800  $\text{cm}^{-1}$  will not be shown. On the other hand, the region containing the  $\nu_{\text{AlO}}$  and  $\nu_{\text{AlCl}}$  modes is illustrated in Figure 1, where very weak signals between 510 and 360  $\text{cm}^{-1}$  are seen along with intense bands going from 349 to 271  $\text{cm}^{-1}$ . It is important to stress that many of these components were not earlier identified by using a laser power of 0.5 W [13]. For instance, the weakest Raman signal of  $[\text{AlCl}_4]^-$  at 492  $\text{cm}^{-1}$ , which is assigned to the asymmetric ClAlCl stretching mode,  $\nu_{\text{as}(\text{ClAlCl})}$ , can be now observed in the spectra. The symmetric vibration ( $\nu_{\text{s}(\text{ClAlCl})}$ ) located at 349  $\text{cm}^{-1}$ , which was previously observed and is the most intense band in this region, is accompanied by another appreciable intensity band at 330  $\text{cm}^{-1}$  (Figure 1(a)), besides others at 286 and 271  $\text{cm}^{-1}$ . The former band is attributed to the  $\nu_{\text{s}(\text{ClAlCl})}$  mode of  $\text{AlCl}_3 \cdot \text{THF}$  and  $\text{AlCl}_3 \cdot 2\text{THF}$  [11,12,14,15], whereas the second belongs to the solvent (Figure S1). The third is reported for the first time in the literature and may be due to the presence of a cationic complex. Regarding the fact that charged species are favored by dilution [13], a known amount of water was further added to the  $\text{AlCl}_3$ -THF system (details are mentioned in Materials and Methods). As can be seen in Figure 1(b), the 330  $\text{cm}^{-1}$  band has its intensity significantly reduced, whereas the bands at 349 and 271  $\text{cm}^{-1}$  are enhanced. Furthermore, the band intensity ratio ( $I_{271}/I_{349} = 0.4$ ) is the same in the absence and presence of water, thus suggesting that only one of the equilibria above (reactions (1) and (2)) takes place. A moderate-intensity Raman band at 284  $\text{cm}^{-1}$  was assigned by Derouault and Forel [11] to the  $\nu_{\text{s}(\text{ClAlCl})}$  mode of solid

$\text{AlCl}_3 \cdot 2\text{THF}$  in an  $[\text{AlCl}_2(\text{THF})_4]^+$ ,  $[\text{AlCl}_4]^-$ -type ionic arrangement. Since bond distances are overall longer in solution, the  $271 \text{ cm}^{-1}$  band could be then related to the monovalent cationic  $\text{Al}(\text{III})$  complex.

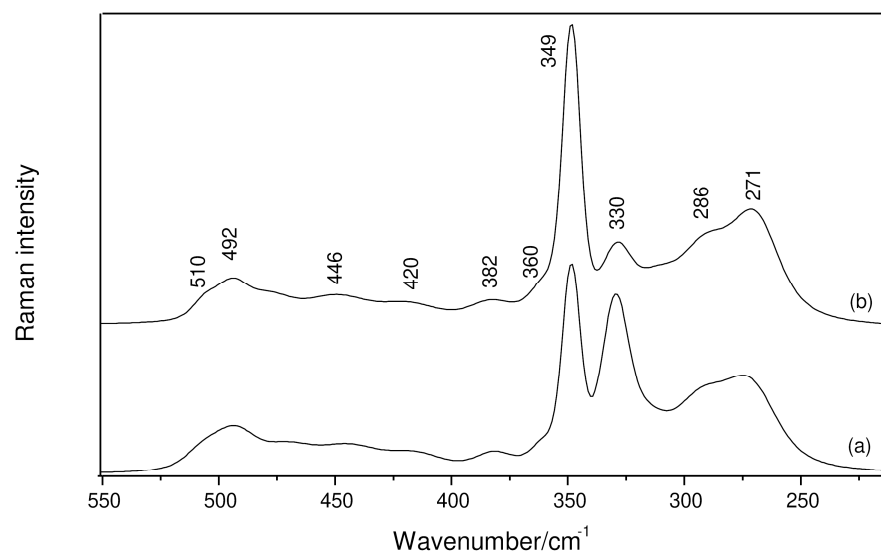


**Figure 1.** Raman spectra of a  $0.5 \text{ mol kg}^{-1}$   $\text{AlCl}_3$  solution at the region of the  $\nu_{\text{AlO}}$  and  $\nu_{\text{AlCl}}$  vibrations: (a)  $\text{AlCl}_3$ -THF system; (b)  $\text{AlCl}_3$ -THF: $\text{H}_2\text{O}$  system with water/salt molar ratio of 0.4.

Far-IR spectra of the same solutions were also obtained and are shown in Figure 2. As expected, the  $491 \text{ cm}^{-1}$  band of  $[\text{AlCl}_4]^-$  is now the most intense one in the considered spectral range, whereas the  $349 \text{ cm}^{-1}$  signal is IR-inactive. The former comes along with a satellite at  $522 \text{ cm}^{-1}$ , which is attributed to the  $\nu_{\text{AlO}}$  mode [16,17] of both neutral and cationic complexes. However, the band related to THF at  $287 \text{ cm}^{-1}$  (Figure S1) is single, and the  $271 \text{ cm}^{-1}$  signal cannot be identified in the absence (Figure 2(a)) and presence (Figure 2(b)) of water, strongly indicating the abundance of a *trans*- $[\text{AlCl}_2(\text{THF})_4]^+$  complex in the media. The intensity of the band at  $331 \text{ cm}^{-1}$  is again decreased as water is added to the system, and this behavior is also observed for a band at  $420 \text{ cm}^{-1}$ . In contrast, the  $405 \text{ cm}^{-1}$  band, which appears as a shoulder in the water-free system, becomes more intense than the component on the higher wavenumber side.

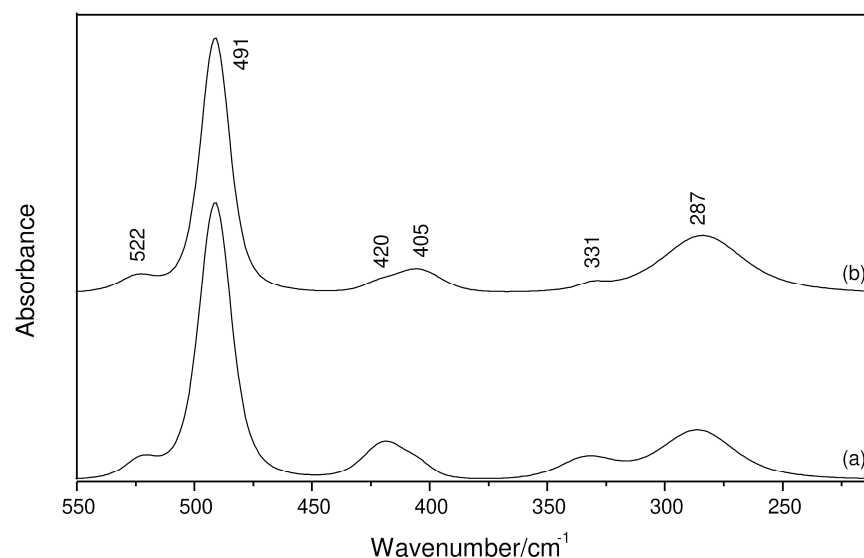


**Figure 2.** Far-IR spectra of a  $0.5 \text{ mol kg}^{-1}$   $\text{AlCl}_3$  solution at the region of the  $\nu_{\text{AlO}}$  and  $\nu_{\text{AlCl}}$  modes: (a)  $\text{AlCl}_3$ -THF system; (b)  $\text{AlCl}_3$ -THF: $\text{H}_2\text{O}$  system with water/salt molar ratio equal to 0.4.

### 2.1.2. AlCl<sub>3</sub>-G4 System

The perturbation of AlCl<sub>3</sub> to the coordination sites of G4 (CO oscillator) is vibrationally characterized by Raman bands at 840 and 870 cm<sup>-1</sup>, which have already been reported by Kitada and colleagues [10]. Here, special attention is paid to Raman bands at 420, 400 and 320 cm<sup>-1</sup>, which also behave in different ways when G4 is employed as a solvent (Figure 3). That is, the first pair of bands has the increased intensity along with the most intense band of [AlCl<sub>4</sub>]<sup>-</sup>, but the latter signal is smoothly decreased with increasing salt molality. Such a trend indicates the presence of an equilibrium between cationic and neutral complexes, where the wavenumber observed for the non-charged species is now downshifted by 10 cm<sup>-1</sup> due to the chelating effect of G4, which weakens the AlCl oscillator. The use of this solvent leads to the appearance of the bands at 550 and 280 cm<sup>-1</sup> (Figure S2) and, as can be seen, the lower wavenumber component would make hard the identification of the band observed at 271 cm<sup>-1</sup> ([AlCl<sub>2</sub>]<sup>+</sup>) in the presence of THF.

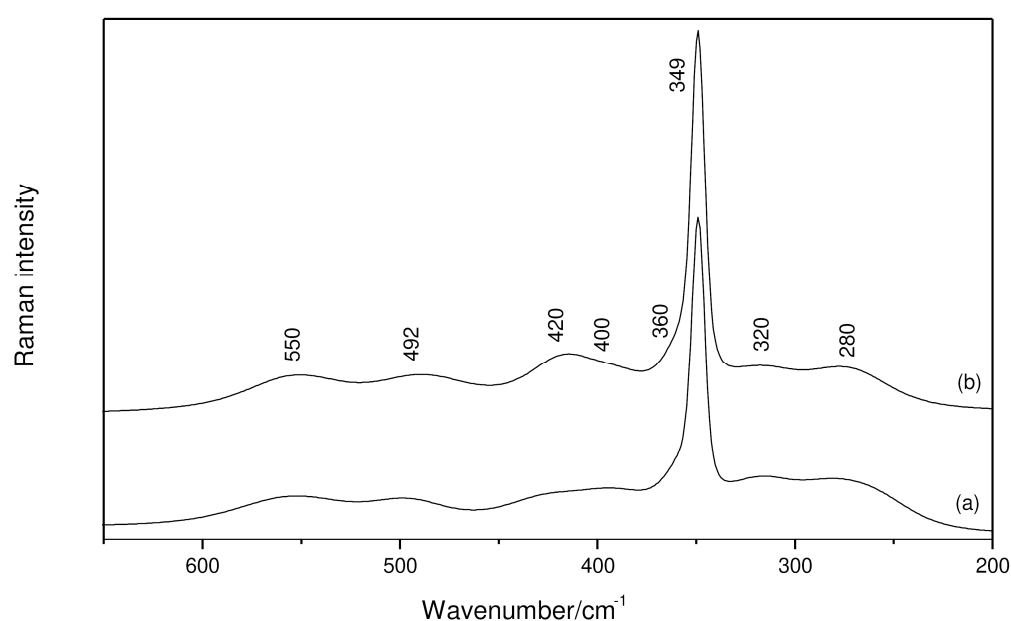


**Figure 3.** Raman spectra of AlCl<sub>3</sub>/G4 solutions at the region of the  $\nu_{\text{AlO}}$  and  $\nu_{\text{AlCl}}$  vibrations: (a) 1 mol kg<sup>-1</sup>; (b) 2 mol kg<sup>-1</sup>.

Evidence for the chemical bond formation between the aluminum halide and G4 is here given by the  $\nu_{\text{AlO}}$  vibration, which arises in the IR spectra as a band at 524 cm<sup>-1</sup> (Figure 4). It is accompanied by a single signal at 491 cm<sup>-1</sup> ([AlCl<sub>4</sub>]<sup>-</sup>) at the 1 mol kg<sup>-1</sup> composition (Figure 4a), but three new bands at 425, 405 and 350 cm<sup>-1</sup> compose the spectrum of the 2 mol kg<sup>-1</sup> AlCl<sub>3</sub>/G4 solution (Figure 4b). One clearly observes a good relationship between the first two bands and those identified at 420 and 400 cm<sup>-1</sup> in the Raman spectra, and the third feature must be overlapped by the strong signal of the anion (Figure 3). As also evidenced by the <sup>27</sup>Al NMR spectra [8,10], the neutral Al(III) species is not observed in the IR spectra, thus confirming that charged complexes are the most abundant in glymes and ruling out any need to add water to this system.

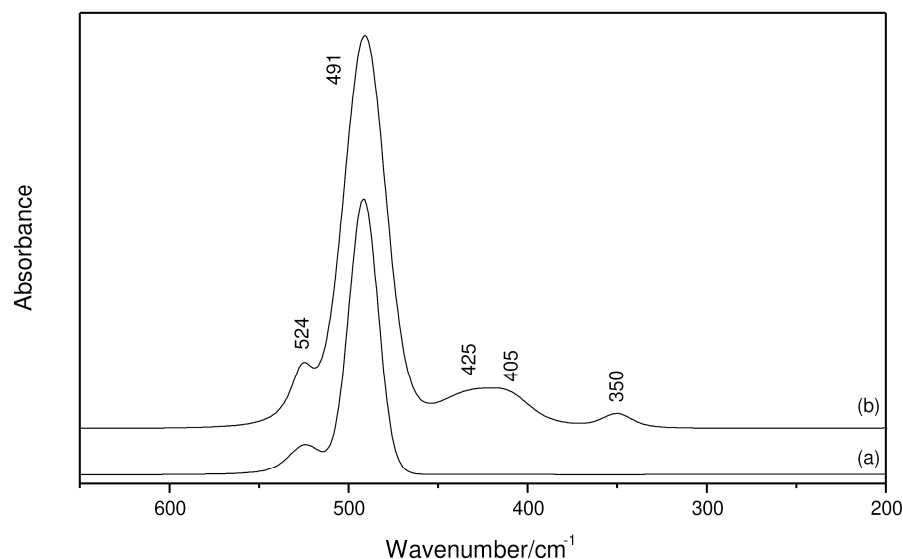


**Figure 4.** Far-IR spectra of  $\text{AlCl}_3/\text{G4}$  solutions at the region of the  $\nu_{\text{AlO}}$  and  $\nu_{\text{AlCl}}$  vibrations: (a)  $1 \text{ mol kg}^{-1}$ ; (b)  $2 \text{ mol kg}^{-1}$ .

## 2.2. Simulated Spectra

From AIMD simulations (details in Materials and Methods), Raman and IR spectra of  $\text{AlCl}_n$  complexes in THF were calculated and are shown in the Figure 5a,b, respectively, and their optimized structures are illustrated in Figure S3. Strong Raman activity at  $\sim 320 \text{ cm}^{-1}$  is predicted for the  $\text{AlCl}_3(\text{THF})$  and planar  $\text{AlCl}_3(\text{THF})_2$  complexes, whereas several weaker bands are obtained for the pyramidal  $\text{AlCl}_3(\text{THF})_2$  structure (“planar” and “pyramidal” refer to the  $\text{AlCl}_3$  core in the complexes). A sole peak at  $420 \text{ cm}^{-1}$  in the IR spectrum of  $\text{AlCl}_3(\text{THF})$  may be correlated to a weaker Raman band calculated at  $416 \text{ cm}^{-1}$ . The binding of the second THF molecule leads to the arising of two moderate signals at  $273 \text{ cm}^{-1}$  and  $356 \text{ cm}^{-1}$  in the IR spectra of planar and pyramidal  $\text{AlCl}_3(\text{THF})_2$ , respectively. The formation of the former complex is slightly disfavored ( $\Delta G_f = 0.5 \text{ kcal/mol}$  for THF binding, i.e., at the limit of the accuracy of calculations), whereas the cost for the formation of the latter is higher and reaches  $4 \text{ kcal/mol}$ . The  $[\text{AlCl}(\text{THF})_5]^{2+}$  complex exhibits a peak at  $452 \text{ cm}^{-1}$ , which is weak in the Raman spectrum and strong in the IR one; a weaker IR band positioned at  $380 \text{ cm}^{-1}$  can be still identified. An intense Raman peak at  $280 \text{ cm}^{-1}$  was calculated for the *trans*- $[\text{AlCl}_2(\text{THF})_4]^+$  complex, and due to its nearly centrosymmetric structure, no IR intensity is obtained in this wavenumber, so that only bands at  $\sim 350$  and  $450 \text{ cm}^{-1}$  appear in the spectrum. On the other hand, the Raman activity of *cis*- $[\text{AlCl}_2(\text{THF})_4]^+$  is spread over some rather weak bands, and its strongest IR signal is calculated at  $408 \text{ cm}^{-1}$ . Although its free energy is about  $8 \text{ kcal/mol}$  higher than that of the *trans* aggregate, their relative stabilities show dependence on the presence of the counterion. The free energy difference between the *cis* and *trans*  $[\text{AlCl}_2(\text{THF})_4][\text{AlCl}_4]$  aggregates drops to  $2.7 \text{ kcal/mol}$ , and the potential energy of the *cis* form is now  $0.2 \text{ kcal/mol}$  lower than the one of the *trans* structures. The effect can be attributed to the better electrostatic stabilization of the *cis* complex, in which, unlike the *trans* aggregate, the  $[\text{AlCl}_4]^-$  anion can be located away from the negatively charged Cl atoms of the  $\text{AlCl}_2$  moiety (Figure S4). QC-calculated vibrational spectra for both isomers with and without the counterion exhibit very similar patterns, except for the presence of the anion bands (Figure S5). So, analogous behavior is also expected for the AIMD-simulated spectra.

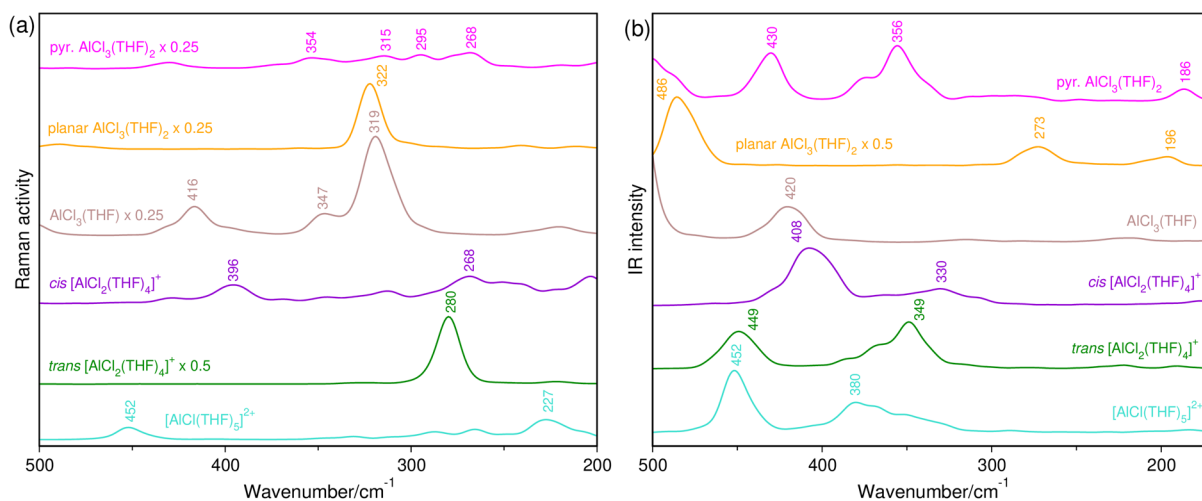


**Figure 5.** AIMD-simulated Raman (a) and IR (b) spectra of  $\text{AlCl}_n$  complexes with explicit THF solvent molecules.

Vibrational spectra simulated for ion aggregates in G4 are shown in Figure 6, and their corresponding structures are available in Figure S6. Intense bands at  $\sim 450$  (Raman spectrum) and  $\sim 490$   $\text{cm}^{-1}$  (IR spectrum) characterize the  $[\text{AlCl}(\text{G4})]^{2+}$  species. The Raman spectra of  $[\text{AlCl}_2(\text{G4})]^+$ , in the *cis* and *trans* forms, show a major band at about  $430$   $\text{cm}^{-1}$ , but a shoulder at  $\sim 400$   $\text{cm}^{-1}$  can be seen for the former. Additional IR information reveals that a very strong signal at around  $450$   $\text{cm}^{-1}$  is characteristic of the second isomer. The charged *trans* structure is only  $0.5$  kcal/mol lower than the *cis* form, so that the free energy difference at the level of calculations is almost negligible. With the presence of the  $[\text{AlCl}_4]^-$  anion, the free energy of the *cis* form becomes  $3.7$  kcal/mol lower than that of the *trans* complex, indicating the better stability of the former structure.

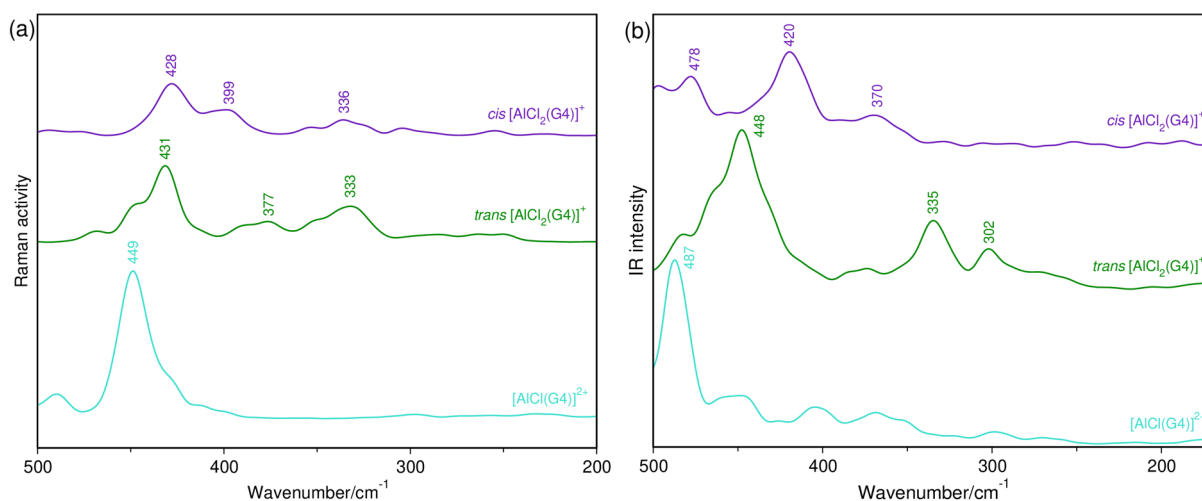


**Figure 6.** AIMD-simulated Raman (a) and IR (b) spectra of  $\text{AlCl}_n$  complexes with explicit G4 solvent molecule.

During this investigation the behavior of the experimental Raman band at  $360$   $\text{cm}^{-1}$ , which is seen in both ethers, has attracted our attention. That is, its inactivity in the IR spectra comes along with the most intense band of  $[\text{AlCl}_4]^-$  at  $349$   $\text{cm}^{-1}$ . Furthermore, it is insensitive to the solvent change and this fact strongly suggests that no ether molecule is coordinated to Al(III). In order to elucidate such spectral behavior, harmonic and anharmonic Raman spectra were calculated for the tetrahedral anion (Figure 7). The four bands predicted by symmetry are present in both spectra, but only one intense signal at

341  $\text{cm}^{-1}$  is observed in the harmonic model for the  $\nu_1$  region (Figure 7a). Unlike, the highest signal of this anion at 339  $\text{cm}^{-1}$  is accompanied by a very weak peak at 353  $\text{cm}^{-1}$  in the anharmonic spectrum (Figure 7b). The latter model is in excellent agreement with the experimental result and allows us to guarantee that the 360  $\text{cm}^{-1}$  band corresponds to the overtone ( $2\nu_4$ ) of the experimental band located at 180  $\text{cm}^{-1}$ .

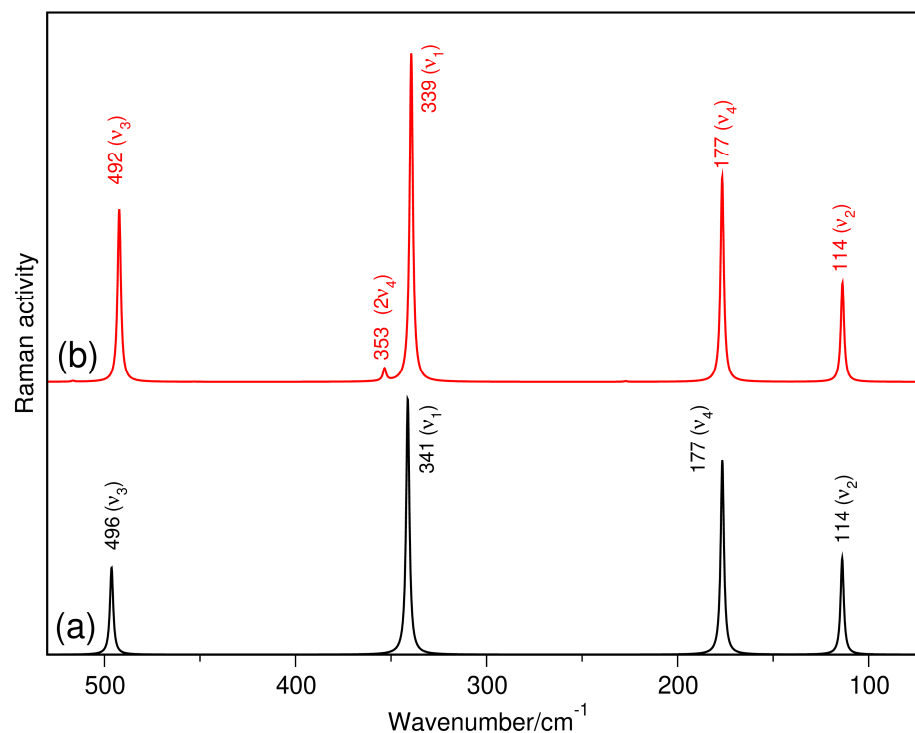


**Figure 7.** Calculated harmonic (a) and anharmonic (b) Raman spectrum of the  $[\text{AlCl}_4]^-$  anion.

### 3. Discussion

The extremely low Raman-scattering cross sections and the IR bands simulated at 430 and 356  $\text{cm}^{-1}$  indicate that the formation of the pyramidal  $\text{AlCl}_3(\text{THF})_2$  complex is unlikely, and such findings are also corroborated by its value of  $\Delta G_f$ . Actually, the experimental and calculated spectra reveal that  $\text{AlCl}_3(\text{THF})$  is the major neutral complex in solution, but tiny amounts of planar  $\text{AlCl}_3(\text{THF})_2$  may be still present. In other words, the theoretical Raman peak at around 320  $\text{cm}^{-1}$ , which is the most intense feature of both complexes, is in line with the experimental Raman band observed at 330  $\text{cm}^{-1}$ , which is also IR-active, and its intensity is strongly dependent on the dilution. Similar dependence can also be seen for a 420  $\text{cm}^{-1}$  band, which is simulated at 416 and 420  $\text{cm}^{-1}$  in the respective Raman and IR spectra of the tetrahedral neutral complex. Since no peak has been calculated at these positions for the bipyramidal neutral compound, we believe that it is either absent or its concentration is too low. If the latter condition is true, its most intense IR peak at 486  $\text{cm}^{-1}$  will be overlapped by the 491  $\text{cm}^{-1}$  band of the  $[\text{AlCl}_4]^-$  anion. Despite our argument, Derouault et al. [12] have reported very strong and medium IR peaks at 490 and 420  $\text{cm}^{-1}$ , respectively, for a *trans*- $\text{AlCl}_3 \cdot 2\text{THF}$  isomer.

The 271  $\text{cm}^{-1}$  band is so related to the  $[\text{AlCl}_2(\text{THF})_4]^+$  species not only because it is enhanced by dilution, but also due to its good relationship with the band simulated at 280  $\text{cm}^{-1}$  for the *trans* isomer. Its high intensity in the Raman spectrum as well as inactivity in the IR one is expected for a totally symmetric vibration. At the same time, the 405  $\text{cm}^{-1}$  band, which is also dependent on the dilution, is IR-active and Raman-inactive, and so it could be assigned to the asymmetric vibration of such an isomer. Nevertheless, it shows good correlation with a peak calculated at 408  $\text{cm}^{-1}$ , which actually belongs to the *cis* isomer. Taking into account that the free energy difference in the isomers in the

presence of  $[\text{AlCl}_4]^-$  suggests the coexistence of both *trans* and *cis* forms in solution, their Raman-scattering and IR-absorption cross sections seem to be then determining for this case. Indeed, the  $280\text{ cm}^{-1}$  band reveals that the *trans* isomer is a better scatterer than the *cis* form, but the latter is a greater absorber, as pointed out by the  $408\text{ cm}^{-1}$  band. Similar trends are also observed from QC-calculated IR and Raman spectra (Figure S5).

The majority presence of both anionic and cationic complexes in G4-based systems is here evidenced by vibrational spectroscopy for the first time. The asymmetric IR band measured at  $425\text{ cm}^{-1}$  shows good relationship with the asymmetric IR peak simulated at  $420\text{ cm}^{-1}$ , whereas the Raman bands observed at  $420$  and  $400\text{ cm}^{-1}$  are very well described by the Raman signals calculated at  $428$  and  $399\text{ cm}^{-1}$  for *cis*- $[\text{AlCl}_2(\text{G4})]^+$ . These results combined with the  $\Delta G_f$  value of this isomer, in the presence of the counterion, strongly suggest its abundance in the investigated solutions.

Comparison between the calculated and experimental data leads to the conclusion that the spectral features of  $[\text{AlCl}]^{2+}$  are not observed in either solvent. Therefore, an appreciable abundance of the doubly charged complex is rather unlikely, thus minimizing the practical importance of the equilibrium (2) in ether-containing electrolytes. Although the chelating effect of the glyme stabilizes the ionic species, the low dielectric constant values of THF and G4, which are very close to each other (see Computational Details), are not capable of providing higher oxidation state species. Our statement is supported by a study of  $\text{AlCl}_3/\text{acetonitrile}$  solutions [18], in which the  $[\text{AlCl}(\text{CH}_3\text{CN})_5]^{2+}$  and  $[\text{Al}(\text{CH}_3\text{CN})_{5-6}]^{3+}$  complexes are proposed from vibrational and  $^{27}\text{Al}$  and  $^{35}\text{Cl}$  NMR spectroscopies. In spite of the higher dielectric constant of the nitrile (36.7), reliable conclusions were not reached due to the large vibrational band overlapping and difficulties in recording accurate NMR data.

The anharmonic Raman spectrum calculated for  $[\text{AlCl}_4]^-$  was very useful in the assignment of the  $360\text{ cm}^{-1}$  band ( $2\nu_4$ ), which is usually identified as a shoulder on the higher wavenumber side of the most intense band ( $\nu_1$ ) of this anion. Here, it is important to mention its presence in the Raman spectra of MACC-based electrolytes [3,5,6,8], which has been assigned to the  $\nu_{\text{MgO}}$  vibration of soluble Mg(II) complexes [16,17]. However, our investigation clearly shows that both  $\nu_{\text{MgO}}$  and  $2\nu_4$  modes compose the shoulder observed in the Raman spectra of those electrolytic solutions.

All the bands discussed in this work are summarized in Tables 1 and 2 for convenience.

**Table 1.** Wavenumbers (in  $\text{cm}^{-1}$ ) of vibrational bands measured and calculated for species present in the  $\text{AlCl}_3$ -THF and  $\text{AlCl}_3$ -THF:H<sub>2</sub>O systems.

Experimental		Calculated		Chemical Species
Raman	IR	Raman	IR	
271		280		<i>Trans</i> - $[\text{AlCl}_2(\text{THF})_4]^+$
286	287			THF solvent
		319		$\text{AlCl}_3(\text{THF})$
330	331	322		<i>Planar</i> - $\text{AlCl}_3(\text{THF})_2$
349		339		$[\text{AlCl}_4]^-$
360		353		$[\text{AlCl}_4]^-$
382				N.A. <sup>1</sup>
	405		408	<i>Cis</i> - $[\text{AlCl}_2(\text{THF})_4]^+$
420	420	416	420	$\text{AlCl}_3(\text{THF})$
446				N.A. <sup>1</sup>
492	491	492	492	$[\text{AlCl}_4]^-$
510				N.A. <sup>1</sup>
				$\text{AlCl}_3(\text{THF})$
	522			<i>Planar</i> - $\text{AlCl}_3(\text{THF})_2$
				<i>Cis</i> - $[\text{AlCl}_2(\text{THF})_4]^+$

<sup>1</sup> N.A. = Not assigned.

**Table 2.** Wavenumbers (in  $\text{cm}^{-1}$ ) of vibrational bands measured and calculated for species present in  $\text{AlCl}_3/\text{G4}$  solutions.

Experimental		Calculated		Chemical Species
Raman	IR	Raman	IR	
280				G4 solvent
320				$\text{AlCl}_3(\text{G4})$
349		339		$[\text{AlCl}_4]^-$
	350		370	$\text{Cis-}[\text{AlCl}_2(\text{G4})]^+$
360		353		$[\text{AlCl}_4]^-$
400	405	399		$\text{Cis-}[\text{AlCl}_2(\text{G4})]^+$
420	425	428	420	$\text{Cis-}[\text{AlCl}_2(\text{G4})]^+$
492	491	492	492	$[\text{AlCl}_4]^-$
	524			$\text{Cis-}[\text{AlCl}_2(\text{G4})]^+$
550				G4 solvent

## 4. Materials and Methods

### 4.1. Experimental Details

Tetrahydrofuran (THF,  $\geq 99.9\%$ ), tetraethylene glycol dimethyl ether (tetraglyme (G4),  $\geq 99\%$ ) and aluminum trichloride ( $\text{AlCl}_3$ , 99.99%) were purchased from Sigma-Aldrich, St. Louis, MO, USA. Salt compositions are expressed as molalities in order to better compare with systems already studied. As pointed out from the composition-dependent Raman spectra, the dissociation degree at a  $0.5 \text{ mol}\cdot\text{kg}^{-1}$   $\text{AlCl}_3/\text{THF}$  solution is substantially high [13]. Hence, such a composition was chosen for analysis, followed by the addition of water in order to obtain a maximum water/salt molar ratio equal to 0.4. Larger quantities of the protic solvent make the solution turbid due to the formation of aluminum hydroxides. No water was delivered to  $\text{AlCl}_3/\text{G4}$  solutions because the glyme stabilizes the ionic species in a certain degree [8–10].

Far-IR spectra were recorded on a Bruker FTIR Vertex 80v spectrometer using polyethylene windows. Raman spectra were acquired on a Bruker FT-Raman MultiRAM using the 1064 nm line of the Nd:YAG laser with power equal to 1 W. A Ge detector operating at liquid nitrogen temperature was also employed, and the solutions were inserted into sealed NMR tubes. Both far-IR and Raman spectra were obtained with  $2 \text{ cm}^{-1}$  resolution at the temperature of  $25 \pm 2 \text{ }^\circ\text{C}$ .

### 4.2. Computational Details

Quantum chemical computations using the Gaussian 09 rev. D01 program [19] were employed to obtain optimized geometries of solvated neutral or ion aggregates and vibrational frequencies. DFT methodology with  $\omega\text{B97XD}$  functional and aug-cc-pVDZ basis set was applied. Complexes of Al(III) cations with Cl anions were explicitly solvated with a few (1–5) solvent (THF or G4) molecules. To account for the bulk solvent, all structures were embedded in an implicit solvent modeled via the Polarizable Continuum Model (PCM) approach. Values of 7.43 and 7.80 were used for static dielectric constant of THF and G4, respectively. Gibbs free energies of solvated aggregates were calculated based on the energies and vibrational frequencies of the optimized structures.

Additional QC calculations of harmonic and anharmonic vibrational frequencies were performed for  $[\text{AlCl}_4]^-$  anion in vacuum at the  $\omega\text{B97XD}/6\text{-}31\text{+G}^*$  level of theory using Gaussian 16 rev. A.03 [20].

Ab initio molecular dynamics simulations were performed for selected solvated ion complexes. Terachem v. 1.93 [21] running on NVIDIA Tesla K40d GPUs was used with  $\omega\text{B97X}$  functional and the  $6\text{-}31\text{+G}^*$  basis set. Implicit solvent was modeled via the COSMO approach using the same values of dielectric constant as in QC calculations. All systems were initially equilibrated in 10 ps simulations with a time step of 1 fs at  $T = 298 \text{ K}$  using the Langevin thermostat. Then, MD simulations in the NE ensemble continued for another 20 ps with a time step of 0.5 fs. IR and Raman spectra were computed as Fourier transforms

of the autocorrelation function of the total dipole moment and the polarizability tensor, respectively, calculated for every second frame of the NE trajectory (i.e., with a time step of 1 fs).

## 5. Conclusions

The use of an FT-Raman instrument with maximum laser power (1W) allowed us to characterize the bands of the  $[\text{AlCl}_2]^+$  cation in  $\text{AlCl}_3$ -containing ethereal solutions. By combining such results with far-IR data and theoretical investigations by QC-calculations and AIMD simulations, it was possible to obtain a conclusion on the main species in the media, and a good relationship with information obtained by  $^{27}\text{Al}$  NMR spectrometry was reached. In THF, appreciable amounts of  $\text{AlCl}_3(\text{THF})$ , besides  $[\text{AlCl}_4]^-$  and the monovalent cationic complex, in the *cis* and *trans* forms, were identified, whereas the *cis* isomer and the anion were the most abundant in G4. The absence of the  $[\text{AlCl}]^{2+}$  cation was interpreted on the basis of the low dielectric constant values of the selected ethers, but further investigations in the presence of higher dielectric constant additives may lead to the formation of this species. Indeed, such a strategy has been used to improve the electrochemical performance of rechargeable Mg battery electrolytes [22] and is also in our plans. Finally, regarding the fact that the Raman technique has been very exploited in the materials science area, the band at  $271\text{ cm}^{-1}$  may be then used as a marker to monitor the presence of  $[\text{AlCl}_2]^+$ , which is deemed a deleterious species for the Mg anode.

**Supplementary Materials:** The following supporting information can be downloaded at: <https://www.mdpi.com/article/10.3390/molecules29225377/s1>, Figure S1: Raman and IR spectra of liquid THF in the spectral range  $550\text{--}210\text{ cm}^{-1}$ ; Figure S2: Raman and IR spectra of liquid G4 in the spectral range  $650\text{--}200\text{ cm}^{-1}$ ; Figure S3: Structures of  $\text{AlCl}_n$  solvates in THF obtained from the QC calculations at the  $\omega\text{B97XD/aug-cc-pVDZ}$  level; Figure S4: Structures of neutral  $[\text{AlCl}_2]^+$  solvates in THF and in G4 obtained from the QC calculations at the  $\omega\text{B97XD/aug-cc-pVDZ}$  level; Figure S5: IR and Raman spectra of charged and neutral  $[\text{AlCl}_2]^+$  solvates in THF and in G4 obtained from the QC calculations at the  $\omega\text{B97XD/aug-cc-pVDZ}$  level; Figure S6: Structures of  $\text{AlCl}_n$  solvates in G4 obtained from the QC calculations at the  $\omega\text{B97XD/aug-cc-pVDZ}$  level.

**Author Contributions:** Conceptualization, W.A.A. and A.E.; methodology, W.A.A. and A.E.; software, A.E.; validation, W.A.A. and A.E.; formal analysis, W.A.A. and A.E.; investigation, G.P.G., W.A.A. and A.E.; resources, W.A.A. and A.E.; data curation, W.A.A. and A.E.; writing—original draft preparation, W.A.A. and A.E.; writing—review and editing, W.A.A. and A.E.; visualization, W.A.A. and A.E.; supervision, W.A.A. and A.E.; project administration, W.A.A. and A.E.; funding acquisition, W.A.A. All authors have read and agreed to the published version of the manuscript.

**Funding:** This study was financed by the Fundação de Amparo à Pesquisa do Estado de Minas Gerais/FAPEMIG (Grant No APQ-00611-22) and Coordenação de Aperfeiçoamento de Pessoal de Nível Superior/CAPES.

**Institutional Review Board Statement:** Not applicable.

**Informed Consent Statement:** Not applicable.

**Data Availability Statement:** The raw data supporting the conclusions of this article will be made available by the authors on request.

**Acknowledgments:** The authors thank Laboratório de Espectroscopia Molecular-LEM/USP for the far-IR facilities. We also gratefully acknowledge Polish high-performance computing infrastructure PL-Grid (HPC Centre ACK Cyfronet AGH) for providing computer facilities and support within computational grant no. PLG/2023/016895. The study was in part carried out using research infrastructure funded by the European Union in the framework of the Smart Growth Operational Programme, Measure 4.2; Grant No. POIR.04.02.00-00-D001/20, "ATOMIN 2.0—Center for materials research on ATOMIC scale for the INnovative economy".

**Conflicts of Interest:** The authors declare no conflicts of interest. The funders had no role in the design of the study; in the collection, analyses, or interpretation of data; in the writing of the manuscript; or in the decision to publish the results.

## References

1. Couch, D.E.; Brenner, A. A Hydride Bath for the Electrodeposition of Aluminum. *J. Electrochem. Soc.* **1952**, *99*, 234–244. [CrossRef]
2. Doe, R.E.; Han, R.; Hwang, J.; Gmitter, A.J.; Shterenberg, I.; Yoo, H.D.; Pour, N.; Aurbach, D. Novel, electrolyte solutions comprising fully inorganic salts with high anodic stability for rechargeable magnesium batteries. *Chem. Commun.* **2014**, *50*, 243–245. [CrossRef] [PubMed]
3. Eilmes, A.; Alves, W.A. Combining experimental and theoretical vibrational spectroscopy to study magnesium aluminum chloride complex electrolytes. *J. Mol. Liq.* **2021**, *333*, 116053. [CrossRef]
4. Eilmes, A.; Alves, W.A. Theory-experiment partnership applied to the spectroscopic analysis of a promising conditioning-free electrolyte for Mg batteries. *J. Mol. Liq.* **2022**, *350*, 118528. [CrossRef]
5. Eilmes, A.; Alves, W.A. Unraveling the solvates in a diethylene glycol dimethyl ether-based electrolyte: A computational-experimental spectroscopic contribution to Mg battery area. *J. Mol. Liq.* **2022**, *359*, 119251. [CrossRef]
6. Eilmes, A.; Alves, W.A. On the solvation structures formed in conditioning-free MMAC-based electrolytes: A theoretical-experimental spectroscopic insight of interest to Mg battery area. *J. Mol. Liq.* **2023**, *384*, 122199. [CrossRef]
7. Quintanilha, O.B.A.; Alves, W.A.; Eilmes, A. Experimental-computational study on the competition between 1,2-dimethoxyethane and tetrahydrofuran in a MACC-based electrolyte. *J. Mol. Liq.* **2024**, *395*, 123927. [CrossRef]
8. Bieker, G.; Salama, M.; Kolek, M.; Gofer, Y.; Bieker, P.; Aurbach, D.; Winter, M. The Power of Stoichiometry: Conditioning and Speciation of  $MgCl_2/AlCl_3$  in Tetraethylene Glycol Dimethyl Ether-Based Electrolytes. *ACS Appl. Mater. Interfaces* **2019**, *11*, 24057–24066. [CrossRef] [PubMed]
9. Nöth, H.; Rurländer, R.; Wolfigardt, P. An Investigation of  $AlCl_3$  Solutions in Ethers by  $^{27}Al$  NMR Spectroscopy. *Z. Naturforsch. B Chem. Sci.* **1982**, *37*, 29–37. [CrossRef]
10. Kitada, A.; Nakamura, K.; Fukami, K.; Murase, K. Electrochemically active species in aluminum electrodeposition baths of  $AlCl_3$ /glyme solutions. *Electrochim. Acta* **2016**, *211*, 561–567. [CrossRef]
11. Derouault, J.; Forel, M.T. Spectroscopic Investigation of Aluminum Trihalide-Tetrahydrofuran Complexes. 1. Structure and Force Fields of the 1:1 and 1:2 Solid Compounds Formed by Aluminum Chloride or Bromide. *Inorg. Chem.* **1977**, *16*, 3207–3213. [CrossRef]
12. Derouault, J.; Granger, P.; Forel, M.T. Spectroscopic Investigation of Aluminum Trihalide-Tetrahydrofuran Complexes. 2. Solutions of Aluminum Chloride or Bromide in Tetrahydrofuran and in Tetrahydrofuran-Dichloromethane. *Inorg. Chem.* **1977**, *16*, 3214–3218. [CrossRef]
13. Alves, C.C.; Campos, T.B.C.; Alves, W.A. FT-Raman spectroscopic analysis of the most probable structures in aluminum chloride and tetrahydrofuran solutions. *Spectrochim. Acta A Mol. Biomol. Spectrosc.* **2012**, *97*, 1085–1088. [CrossRef] [PubMed]
14. Pour, N.; Gofer, Y.; Major, D.T.; Aurbach, D. Structural analysis of electrolyte solutions for rechargeable Mg batteries by stereoscopic means and DFT calculations. *J. Am. Chem. Soc.* **2011**, *133*, 6270–6278. [CrossRef]
15. See, K.A.; Chapman, K.W.; Zhu, L.; Wiaderek, K.M.; Borkiewicz, O.J.; Barile, C.J.; Chupas, P.J.; Gewirth, A.A. The interplay of Al and Mg speciation in advanced Mg battery electrolyte solutions. *J. Am. Chem. Soc.* **2016**, *138*, 328–337. [CrossRef]
16. Pye, C.C.; Rudolph, W.W. An ab initio and Raman investigation of magnesium(II) hydration. *J. Phys. Chem. A* **1998**, *102*, 9933–9943. [CrossRef]
17. Rudolph, W.W.; Irmer, G.; Hefter, G.T. Raman spectroscopic investigation of speciation in  $MgSO_4(aq)$ . *Phys. Chem. Chem. Phys.* **2003**, *5*, 5253–5261. [CrossRef]
18. Dalibart, M.; Derouault, J.; Granger, P.; Chapelle, S. Spectroscopic Investigations of Complexes between Acetonitrile and Aluminum Trichloride. 1. Aluminum Chloride-Acetonitrile Solutions. *Inorg. Chem.* **1982**, *21*, 1040–1046. [CrossRef]
19. Frisch, M.J.; Trucks, G.W.; Schlegel, H.B.; Scuseria, G.E.; Robb, M.A.; Cheeseman, J.R.; Scalmani, G.; Barone, V.; Mennucci, B.; Petersson, G.A.; et al. *Gaussian 09, Revision D.01*; Gaussian, Inc.: Wallingford, CT, USA, 2013.
20. Frisch, M.J.; Trucks, G.W.; Schlegel, H.B.; Scuseria, G.E.; Robb, M.A.; Cheeseman, J.R.; Scalmani, G.; Barone, V.; Petersson, G.A.; Nakatsuji, H.; et al. *Gaussian 16, Revision A.03*; Gaussian, Inc.: Wallingford, CT, USA, 2016.
21. *Terachem*, v. 1.93; PetaChem: Los Altos Hills, CA, USA, 2017. Available online: <http://www.petachem.com/> (accessed on 21 October 2024).
22. Yang, Y.; Wang, W.; Nuli, Y.; Yang, J.; Wang, J. High active magnesium trifluoromethanesulfonate-based electrolytes for magnesium-sulfur batteries. *ACS Appl. Mater. Interfaces* **2019**, *11*, 9062–9072. [CrossRef]

**Disclaimer/Publisher's Note:** The statements, opinions and data contained in all publications are solely those of the individual author(s) and contributor(s) and not of MDPI and/or the editor(s). MDPI and/or the editor(s) disclaim responsibility for any injury to people or property resulting from any ideas, methods, instructions or products referred to in the content.